COMPDYN 2011
III ECCOMAS Thematic Conference on
Computational Methods in Structural Dynamics and Earthquake Engineering
M. Papadrakakis, M. Fragiadakis, V. Plevris (eds.)
Corfu, Greece, 26–28 May 2011

COLLAPSE RESISTANCE OF BUILDINGS WITH LARGE-SCALE MAGENTO-RHEOLOGICAL (MR) DAMPERS

Yunbyeong Chae[1], James M. Ricles[1], and Richard Sause[1]

[1] Lehigh University, 117 ATLSS Drive, Bethlehem, PA 18015 USA
e-mail: yuc206@lehigh.edu, jmr5@lehigh.edu, rs0c@lehigh.edu

Keywords: Magneto-Rheological (MR) damper, Semi-Active Control, Incremental Dynamic Analysis, Collapse Fragility

Abstract. *Supplemental damping systems are known to improve the performance of structures under the design basis earthquake (DBE) and maximum considered earthquake (MCE). In this paper, the seismic collapse potential of a 3-story building with large-scale MR dampers is investigated for extreme levels of ground motion beyond the MCE, where the MR dampers are controlled by various control algorithms. The control algorithms include: i) passive control; ii) linear quadratic regulator (LQR) semi-active control; iii) sliding model control (SMC) semi-active control; iv) decentralized bang-bang (DBB) semi-active control; and v) phase angle control (PAC) semi-active control. The collapse fragility curves of the building with these structural control strategies are obtained using the incremental dynamic analysis (IDA) procedure with an ensemble of ground motions recommended by FEMA P695. The nonlinear time history analysis for the IDA is conducted using OpenSees, where a phenomenological based model to account for strength deterioration in beam plastic hinge regions subject to cyclic loading is incorporated into OpenSees. The collapse fragility curves for various structural control strategies are compared and discussed to assess the performance of the building structure with MR dampers in mitigating structural collapse under extreme earthquake ground motions.*

1 INTRODUCTION

In earthquake engineering, collapse implies that a structural system, or a part of it, is incapable of maintaining gravity load carrying capacity in the presence of seismic effects [1]. When a building is subjected to large story drifts, it is vulnerable to dynamic instability due to P-Δ effects and deterioration in strength and stiffness of its structural components that can lead to collapse of the system. Collapse prevention has always been a major concern in the design of structures. The recently developed FEMA P695 [2] document provides a methodology for seismic collapse assessment of structures.

While several studies have been conducted to assess the performance of supplemental damping systems and their effectiveness in mitigating the seismic hazard of structures under the design basis earthquake (DBE) and maximum considered earthquake (MCE), the collapse resistance of buildings with Magneto-Rheological (MR) dampers has not been investigated. The seismic collapse potential of structures with passive supplemental damping systems has been investigated by a few researchers using the incremental dynamic analysis (IDA) method [4-6]. In this paper, the collapse resistance capacity of a 3-story building with moment resisting frames (MRFs) and braced frames with MR dampers designed to achieve specified performance levels under the DBE and MCE is assessed for seismic collapse using the procedure given in FEMA P695. The nonlinear time history analyses used in the IDA method are conducted using OpenSees [6]. A phenomenological-based model developed by Ibarra and Krawinkler [1] and modified by Lignos [7] for modeling deterioration in beam plastic hinge regions in MRFs is incorporated into OpenSees. IDA are performed on the building for cases involving five different controllers [8]: i) passive control; ii) linear quadratic regulator (LQR); iii) sliding mode control (SMC); iv) decentralized bang-bang control (DBB); and v) phase angle control (PAC). Collapse fragility curves are obtained using the ensemble of 22 recorded far-field ground motion pairs (i.e., 44 far-field ground motions) recommended by FEMA P695. The collapse fragility curves for the various control strategies are compared in order to assess the performance of the MR damper control strategies in mitigating structural collapse under extreme earthquake ground motions.

2 BEAM PLASTIC HINGE DETERIORATION MODEL

The P-Δ effect and the strength and stiffness deterioration of structural components are considered to be the major contributors to the collapse of a structural system under seismic loading. The P-Δ effect is well-understood and mathematical models have been formulated for use in linear and nonlinear structural analysis, while the modeling of strength and stiffness deterioration under seismic loading is an on-going research topic. For the accurate evaluation of the collapse of a structure, it is necessary to construct a model that is capable of capturing the strength and stiffness deterioration of structural components under seismic loading. In this section, recently developed deterioration models for plastic hinges in steel beams of MRFs are introduced. The models are used for the IDA presented later in this paper.

Ibarra and Krawinkler developed a hysteretic inelastic deterioration model to describe the moment-rotation behavior in the plastic hinge region of a steel or concrete beam [1]. The model is based on a backbone curve that defines a reference skeleton behavior of a non-deteriorated system. A set of rules are used to define the basic characteristics of the hysteretic behavior between the bounds defined by the backbone curve as well as deterioration in strength and stiffness with respect to the backbone curve.

Lignos modified the Ibarra-Krawinkler model based on observations from data from several hundred tests that had been conducted on steel and reinforced concrete beams [7]. Lignos modified the backbone curve and the cyclic deterioration formulation in the original Ibarra-

Krawinkler model, where the new backbone curve proposed by Lignos is shown in Figure 1. In Figure 1, δ_c is the cap deformation (deformation associated with capacity F_c for monotonic loading); F_y is the effective yield strength; δ_y is the effective yield deformation (=F_y/K_e); K_e is the effective elastic stiffness; F_r is the residual strength capacity; δ_r is the deformation at the residual strength; δ_u is the ultimate deformation capacity; δ_p is the plastic deformation capacity associated with monotonic loading; δ_{pc} is the post-capping deformation capacity associated with monotonic loading; and κ is the residual strength ratio (=F_r/F_y). The capacity F_c mentioned above is the strength cap associated with the maximum strength incorporating average strain hardening. The strain hardening ratio α_s and the post-capping stiffness ratio α_c are defined as $\alpha_s = K_s/K_e = [(F_c/F_y)/\delta_p]/K_e$ and $\alpha_c = K_{pc}/K_e = (F_c/\delta_{pc})/K_e$, respectively. The reference energy dissipation capacity E_t, which is used to describe the cyclic deterioration, is defined as $E_t = \Lambda\delta_p$, where Λ denotes the reference cumulative deformation capacity.

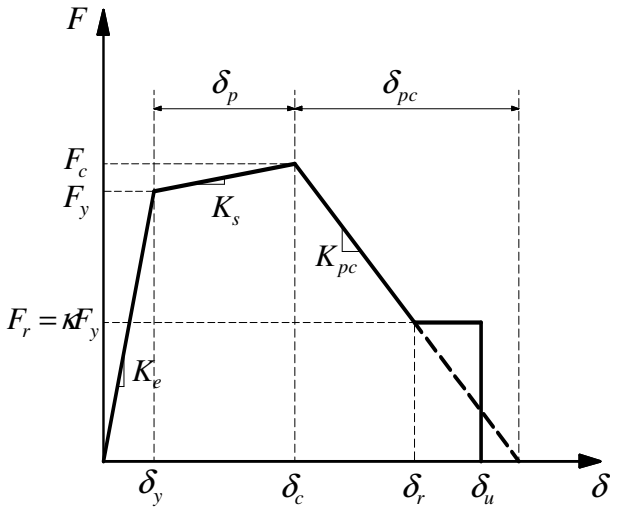

Figure 1 Modified backbone curve of Ibarra-Krawinkler model

3 MODELING OF 3-STORY BUILDING

The 3-story building shown in plan and elevation in Figures 2 and 3, respectively, was used for the study. The building has two perimeter MRFs along each of its sides and braced internal bays with MR dampers (called *damped brace frames* (DBFs)) at the 2nd and 3rd floors. The structure was designed using the simplified design procedure developed by Chae et al. [8] to achieve a performance objective of 1.5% story drift and 2.6% story drift under the DBE and MCE, respectively. The 3-story building was scaled down using a scale factor of 0.6 for the study since a reduced scale model of the building will be constructed and tested in the laboratory in future research studies. The members of the MRF are proportioned using a weak beam-strong column design. Yielding is expected to occur predominately at the ends of the MRF beams and at the base of the columns in the first story of the MRF and DBF under the DBE. The beams and diagonal bracing members in the DBF have pin-ended connections. The beams are axially restrained in the DBF by the floor diaphragm (which is assumed to be rigid in-plane) at each floor level. The inertial force due to the floor mass is transferred to the MRF and DBF through the rigid floor diaphragm connected to the lean-on column depicted in Figure 4. The diagonal bracing is expected to remain elastic up to 135% story drift [9].

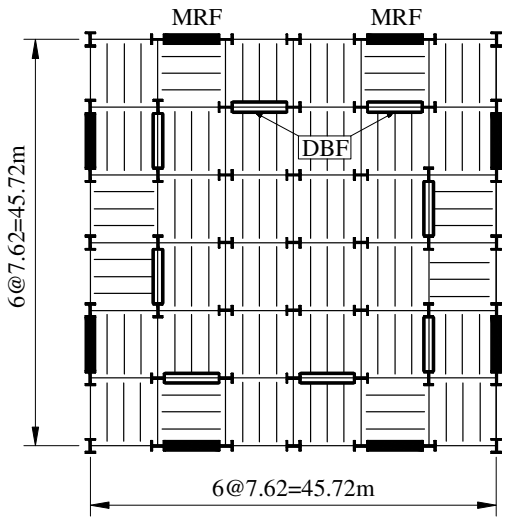

Figure 2 Floor plan of prototype building

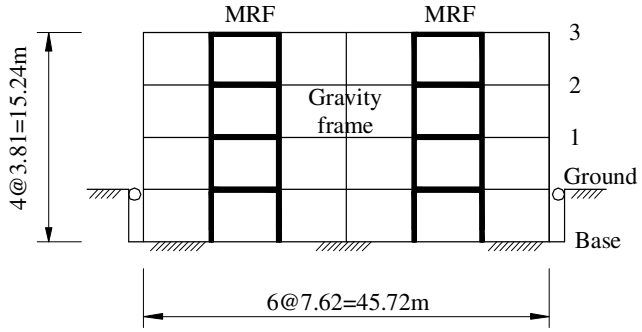

Figure 3 Exterior elevation of prototype building

Table 1 Member sizes for MRFs and gravity frames

Story (or Floor Level)	MRFs		Gravity Frames	
	Column	Beam	Column	Beam
1	W8X67	W18X46	W8X48	W10X30
2	W8X67	W14X38	W8X48	W10X30
3	W8X67	W10X17	W8X48	W10X30

Table 2 Member sizes for DBFs

Story (or Floor level)	Column	Beam	Diagonal bracing
1	W10X33	W10X30	-
2	W10X33	W10X30	W6X20
3	W10X33	W10X30	W6X20

Tables 1 and 2 summarize the member sizes for the 0.6-scale building. The OpenSees model for the scaled building is shown in Figure 4. Symmetry in the floor plan and ground motions along only one principal axis of the building were considered in the analysis. Hence, only one-quarter of the building was modeled consisting of one MRF, one DBF, and the gravity frames that are within the tributary area of the MRF and DBF.

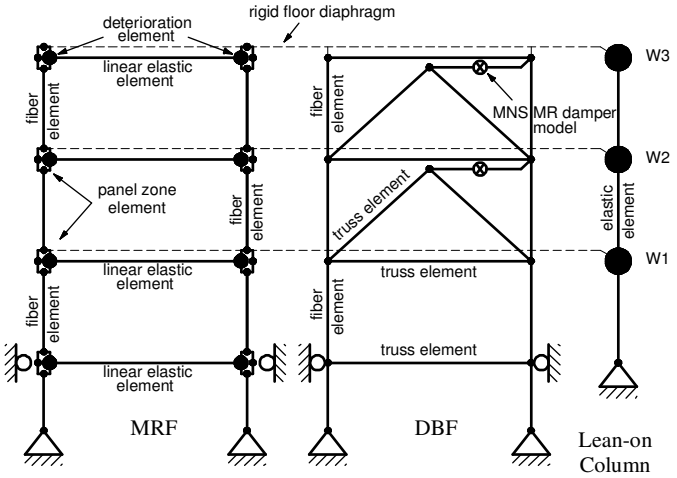

Figure 4 OpenSees model of the 3-story structure for the incremental dynamic analysis

Each beam of the MRF in the model consists of three elements: two inelastic deterioration elements with zero length at the column faces based on the modified Ibarra-Krawinkler model; and one linear elastic element between the deterioration elements. The parameters for the deterioration element are summarized in Table 3, where M_y, θ_p and θ_{pc} denote the yield moment, plastic rotation capacity and the post-capping rotation capacity, respectively. The values of these parameters are based on Lignos and Krawinkler [10] for the beam sections used in the MRF.

Table 3 Parameters for deterioration element for MRF beams

Beam size	Deterioration element parameters						
	K_e (kN-m/m)	M_y (kN-m)	α_s	θ_p (rad)	θ_{pc} (rad)	Λ	κ
W10X17	103531	116	0.002	0.062	0.207	1.244	0.01
W14X38	462520	383	0.002	0.043	0.171	1.084	0.01
W18X46	855748	564	0.002	0.033	0.186	1.104	0.01

The columns of the MRF and DBF are modeled using a nonlinear distributed plasticity force-based beam-column element. Each fiber is modeled with a bilinear stress-strain relationship with a post-yielding stiffness that is 0.01 times the elastic stiffness. The columns extend below the ground level in the model to the base, where they are pinned. The beam-to-column joints in the MRF are modeled using a nonlinear panel zone element, where shear and symmetric column bending deformation modes are considered [11]. Doubler plates in the panel zones of the MRF are included in the model. The beams and braces of the DBF are

modeled using linear elastic truss elements. The gravity frames are idealized using the concept of a lean-on column, where an elastic beam-column element with geometric stiffness is used to model the lean-on column. The section properties of the lean-on column are obtained by taking the sum of the section properties of each column of the gravity frames within the tributary area (i.e., one quarter of the floor plan) of the MRF and the DBF.

The structural model in Figure 4 has two major structural components that can lead to dynamic instability under extreme earthquake ground motions: (1) negative stiffness induced by the gravity loads acting on the lean-on column (the P-Δ effect); and (2) strength deterioration in the inelastic deterioration elements in the beams of the MRF. The columns of the MRF and DBF are assumed to have sufficient strength and compactness of their cross-sections such that no deterioration in strength or stiffness of the columns is expected to occur.

To model a rigid floor diaphragm at each floor level the top node of each panel zone element in the MRF and the beam-column joint in the DBF are horizontally constrained together with the node of the lean-on column, while the vertical and rotational DOFs are released. The MR damper is assumed to be located between the top of the diagonal bracing and beam-to-column joint of the DBF. The variable current MNS model developed by Chae [9] is used to model the MR dampers for the nonlinear time history analysis.

Large-scale MR dampers were used for the study which can generate a 200kN damper force at a velocity of 0.1m/sec. [12]. The damper has a stroke limit of ±279mm. The story height of the 3-story building is 2.286m, implying that the dampers will reach their stroke limit at 12.2% story drift. Since large story drifts can be expected in a collapse simulation, the MR damper may bottom out with respect to the damper stroke limit under extreme earthquake ground motions. In this case, a gap or the hook element should be included in the model to account for the dynamic behavior associated with reaching the stroke limit, as suggested by Miyamoto et al. [5]. The MR dampers in this study are assumed to have sufficient stroke limit to accommodate the large story drifts during a collapse simulation since no experimental data exists that can be used to model the effect of bottoming out of the dampers.

4 GROUND MOTIONS

As noted previously, the far-field ground motion record set recommended by FEMA P695 (ATC 2009) was selected as ground motions for the IDA. These ground motions were selected to permit evaluation of the record-to-record (RTR) variability of the structural response and calculation of the median of the intensity of spectral acceleration at which collapse occurs. Among the 22 earthquakes, 14 occurred in the United States and 7 in other countries. Event magnitudes range from M6.5 to M7.6, with an average magnitude of M7.0. Each earthquake has two horizontal components so that a total of 44 ground motions are used for the IDA.

FEMA P695 recommends the use of spectral acceleration at the fundamental period of a structure, S_{aT_1}, as the intensity measure (IM). The ground motions are scaled up (or down) based on the spectral acceleration at the fundamental period of the structure. The MR damper stiffness depends on its displacement amplitude [9]. Hence, the effective fundamental period of the structure is dependent on the amplitude of the damper displacements, which is a function of the intensity of ground motion. In this paper, the fundamental period of the structure without MR dampers is used to determine the spectral acceleration corresponding to the IM, rather than using the effective fundamental period of the structure with the dampers. The fundamental period without the MR dampers is 0.94 sec [9], and the scaling of ground motions is performed based on the spectral acceleration at this period.

5 CONTROLLERS

As noted previously, five different control strategies for MR dampers are used in this study, namely: i) passive control; ii) linear quadratic regulator (LQR); iii) sliding mode control (SMC); iv) decentralized bang-bang control (DBB); and v) phase angle control (PAC). More details on these controllers can be found in Chae [9]. A constant current with I=2.5A is supplied to the MR dampers for passive control, while for the semi-active controllers the current switched from I=0.0A to 2.5A based on the semi-active control law.

6 INCREMENTAL DYNAMIC ANALYSIS

The incremental dynamic analysis (IDA) curves are a set of plots that correlate a damage measure (DM) with the IM that characterizes the applied scaled accelerograms [13]. The roof drift ratio of the building, θ_{roof}, is selected as the DM for this study. A ground motion is scaled up until dynamic instability occurs, where an IDA curve becomes a flat line, i.e., at collapse. Each selected ground motion is gradually scaled up until θ_{roof} reaches 17% or collapse occurs. For the 44 ground motions in the ensemble, the IDA curves all became flat indicating collapse before θ_{roof} reached 17%. The median roof drift when the IDA curves become flat is approximately 14%.

Figures 5 through 10 show the IDA curves for the structure with various control strategies. These results are for the 44 ground motions. The collapse margin ratio (CMR) was determined for each case, where the CMR is defined by FEMA P695 as the ratio of the median value for the collapse spectral acceleration, $\hat{S}_{CT}$, to the spectral acceleration of the MCE, S_{MT}, at the fundamental period of the structural system:

$$\text{CMR} = \frac{\hat{S}_{CT}}{S_{MT}} \tag{1}$$

$\hat{S}_{CT}$ for each control case is calculated from the IDA curves and marked in Figures 5 through 10 along with the S_{MT}. Table 4 shows the CMR values for each control strategy. Since the purpose is to evaluate the collapse capacity of a structure with MR dampers with various control strategies, the further adjustment of the CMR values based on the spectral shape factor (SSF) [2] is not considered in this study. The results in Table 4 show that when passive control is used that the CMR value increases by about 26% compared to the no damper case, demonstrating the benefit of using MR dampers. The overall performance of each semi-active controller is similar to that of the passive control case, except for the LQR controller. The LQR controller shows the highest CMR value, where the improvement over passive control is about 7%.

7 COLLAPSE FRAGILITY CURVES

A collapse fragility curve is the cumulative distribution function (CDF) which relates the intensity of ground motion to the probability of collapse, and is constructed utilizing the results of the IDAs. For a prescribed level of spectral acceleration S_{aT_1}, the number of cases, N_{SaT1}, where collapse occurs for a spectral acceleration equal to or less than this value of S_{aT_1} among the IDA curves for the various ground motions is counted. The probability of collapse associated with this value of S_{aT_1} is N_{SaT1}/N_{tot}, where N_{tot} is the total number of IDA curves (i.e., ground motions).

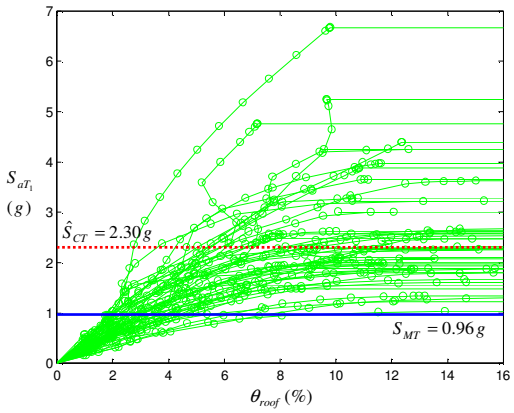

Figure 5 IDA curves: no damper case

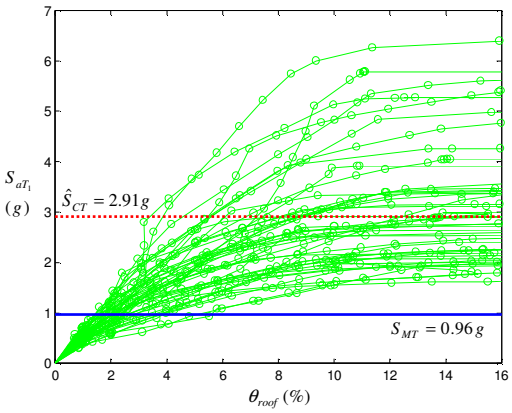

Figure 6 IDA curves: passive control

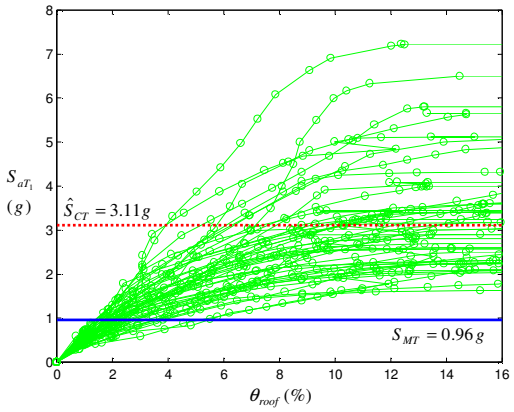

Figure 7 IDA curves: LQR control

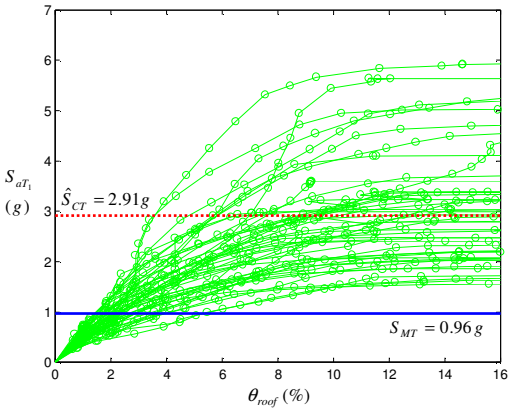

Figure 8 IDA curves: SMC

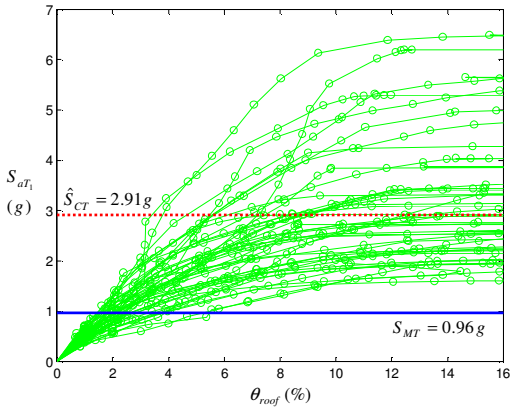

Figure 9 IDA curves: DBB control

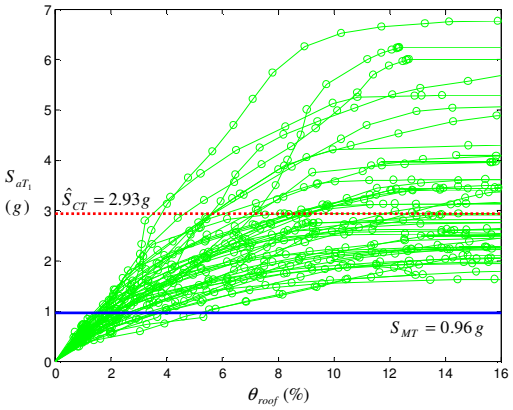

Figure 10 IDA curves: PAC

The probability of collapse typically follows a lognormal distribution. A set of collapse data points can thus be fitted using the lognormal distribution to construct the collapse fragility curve. The fitted lognormal distribution is defined by two parameters, namely, the median collapse spectral acceleration ($\hat{S}_{CT}$), and the standard deviation of the natural logarithm of the collapse spectral accelerations (ζ). The CDF with a lognormal distribution, $F(x)$, is mathematically expressed as

$$F(x) = \int_0^x \frac{1}{s\zeta\sqrt{2\pi}} \exp\left[-\frac{(\ln s - \lambda)^2}{2\zeta^2}\right] ds = \Phi\left(\frac{\ln x - \lambda}{\zeta}\right) \quad (2)$$

where, Φ is the cumulative distribution function of the standard normal distribution and $\lambda = \ln \hat{S}_{CT}$. Figure 11 compares the collapse fragility curves for passive control with the no damper case. The fragility curve for passive control is located to the right of the fragility curve for the no damper case, which means the collapse potential of the structure with passive control is lower than that for the structure with no dampers. This result is also illustrated in Table 4 by a comparison of the CMR values, where passive control has a higher CMR value. The collapse fragility curve for various semi-active control strategies are compared to the collapse fragility curve for passive control in Figures 12 through 15. The collapse fragility curves for the semi-active control strategies are shown to be similar to passive control, except for the LQR controller. The collapse fragility curve for the building with the LQR controller is more notably to the right of that for the passive control case (Figure 12) than for the other comparisons, indicating a lower probability of collapse compared to passive control, and consistent with having a higher CMR value in Table 4.

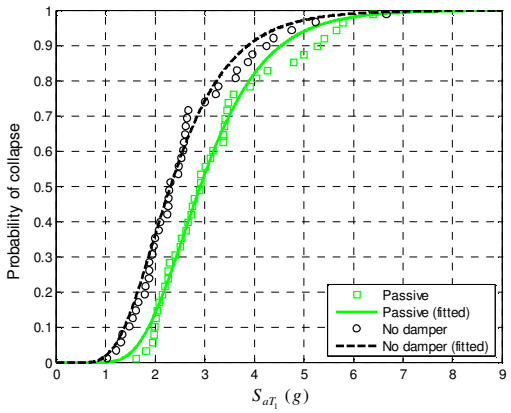

Figure 11 Collapse fragility curves where no damper case is compared with passive control

Table 4 Collapse margin ratio (CMR) for 3-story building with various control strategies

	No damper	Passive	LQR	SMC	DBB	PAC
CMR	2.39	3.02	3.23	3.03	3.02	3.05

8 COLLAPSE MODE

The collapse mode of the building studied is characterized by the formation of plastic hinges in the beams and columns leading to a collapse mechanism. A soft story mechanism, where both ends of all columns at a particular story level develop plastic hinges, did not occur in any of the cases. The design methodology based on a strong column-weak beam design appears to enable a soft story collapse mechanism to be avoided.

Figure 16 shows the deformed shape of the building with passively controlled MR dampers at the time of maximum drift under the 1994 Northridge earthquake (Canyon country, 000 component), where the ground motion was scaled to a spectral acceleration of S_{aT_1}=2.25g. Collapse for this ground motion occurs when S_{aT_1}=2.27g. Both ends of each beam in the 1st through 3rd floors in the MRF and the ground level of the 1st story columns for both the MRF and DBF form plastic hinges during the earthquake.

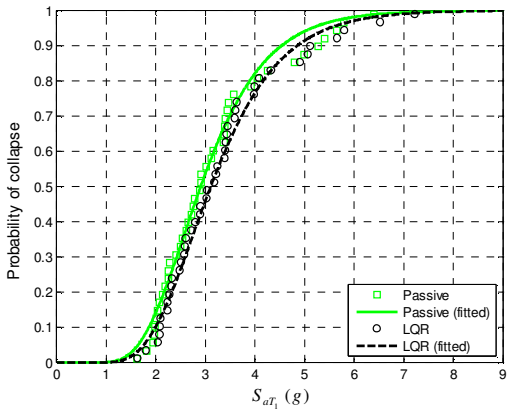

Figure 12 Collapse fragility curves where LQR controller is compared with passive control

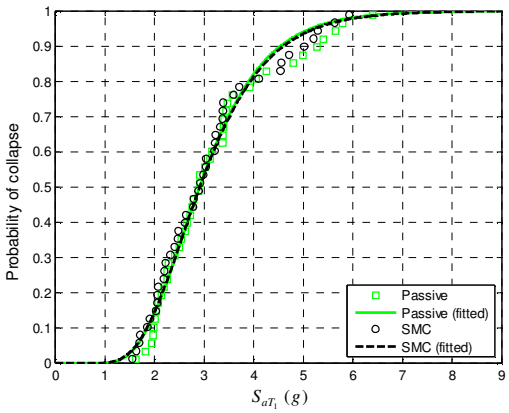

Figure 13 Collapse fragility curves where SMC controller is compared with passive control

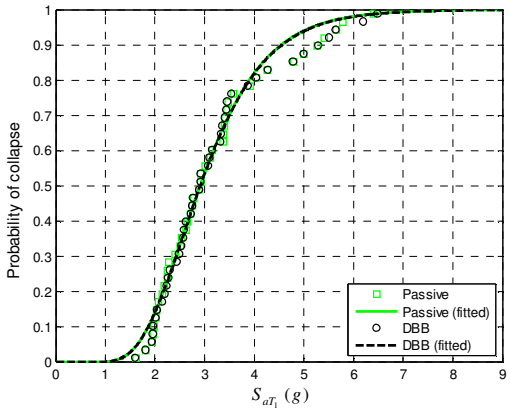

Figure 14 Collapse fragility curves where DBB controller is compared with passive control

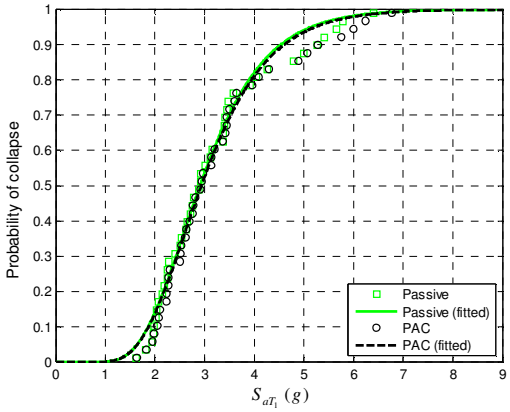

Figure 15 Collapse fragility curves where PAC controller is compared with passive control

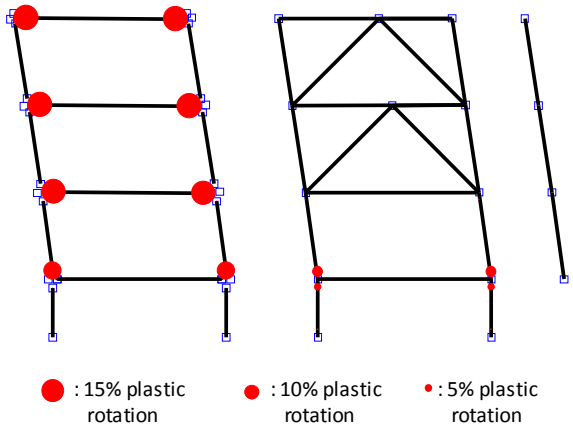

Figure 16 Deformed shape of building at incipient collapse; the solid circles represent the location of plastic hinges and their size denotes the magnitude of plastic rotation

9 CONCLUSIONS

In this paper, the collapse potential of a 3-story steel frame building with MR dampers controlled by various control strategies was investigated. A model of the structure was developed using OpenSees that included strength and stiffness deterioration along with the P-Δ effect. Incremental dynamic analyses based on nonlinear time history earthquake simulations were performed to obtain the statistical response and collapse margin ratios (CMRs) for the structure. Five different control strategies for the MR dampers were used, and the collapse potential for each case was compared. The passive control of MR dampers with a 2.5A constant current input improved the CMR value by about 26% compared to the structure without MR dampers. The collapse fragility curves for sliding mode control, decentralized bang-bang control, and phase angle control resulted in almost the same collapse potential as passive control, while the LQR controller provided a reduction in the collapse potential. The CMR is about 7% greater for the structure with an LQR controller compared to passive control.

The LQR and SMC controllers require control gains to be specified. To reach more general conclusions about the seismic collapse potential of buildings with semi-active controlled MR dampers it is recommended that the effect of the control gains on the collapse potential be further investigated. In addition, other semi-active controllers and various structural geometries (e.g. the height of the building) should be included. The effect of a damper bottoming out on the collapse potential of structures with MR dampers also needs to be investigated.

ACKNOWLEDGEMENTS

This paper is based upon work supported by grants from the Pennsylvania Department of Community and Economic Development through the Pennsylvania Infrastructure Technology Alliance, and by the National Science Foundation under Award No. CMMI-1011534, within the George E. Brown, Jr. Network for Earthquake Engineering Simulation Research (NEESR) program, Award No. CMS-0612661, and Award No. CMS-0402490 NEES Consortium Operation.

REFERENCES

[1] Ibarra, L.F. and Krawinkler, H., Global collapse of frame structures under seismic excitations, *John A. Blume Earthquake Engineering Center, Report No. 152*, 2005.

[2] Applied Technology Council, *Quantification of building seismic performance factors*, ATC-63 Project Report (FEMA P695), Redwood City, CA, 2009.

[3] Solberg, K., Bradley, B., Rodgers, G., Mander, J., Dhakal, R., and Chase, J., Multi-level seismic performance assessment of a damage-protected beam-column joint with internal lead dampers, *New Zealand Society for Earthquake Engineering Annual Conference (NZSEE 07)*, Palmerston North, New Zealand, 2007.

[4] Marshall, J.D. and Charney, F.A., A hybrid passive control device for steel structures, I: development and analysis, *Journal of Constructional Steel Research*, **66**, 1278-1286, 2010.

[5] Miyamoto, H.K., Gilani, A.S.J., Ariyaratana, Ch., and Wada, A., Probabilistic evaluation of seismic performance of steel moment framed buildings incorporating damper limit states, *ASCE Structures Congress*, Orlando, FL, 2010.

[6] OpenSees, *Open system for earthquake engineering simulation*, Pacific Earthquake Engineering Research Center, University of California, Berkeley, 2009.

[7] Lignos, D., Sidesway collapse of deteriorating structural systems under seismic excitations, *Ph.D. Dissertation*, Stanford University, Stanford, CA, 2008.

[8] Chae, Y., Dong, B., Ricles, J.M., and Sause, R., Development of simplified design procedure for structures with magneto-rheological (MR) dampers, *8th International Conference on Urban Earthquake Engineering*, Tokyo, Japan, 2011.

[9] Chae, Y., Seismic hazard mitigation of building structures using magneto-rheological dampers, *Ph.D. Dissertation*, Lehigh University, PA, 2011.

[10] Lignos, D., and Krawinkler, H., Sidesway collapse of deteriorating structural systems under 17 seismic excitations, *John A. Blume Earthquake Engineering Center Report No. TR 172*, Department of Civil Engineering, Stanford University, 2009.

[11] Seo, C.Y., Lin, Y.C., Sause, R, and Ricles, J.M., Development of analytical models for 0.6 scale self-centering MRF with beam web friction devices, *6th International Conference for Steel Structures in Seismic Area (STESSA)*, Philadelphia, 2009.

[12] Chae, Y., Ricles, J.M., and Sause, R., Development of a large-scale MR damper model for seismic hazard mitigation assessment of structures, *9th US National and l10th Canadian Conference on Earthquake Engineering*, Toronto, Canada, 2010.

[13] Vamvatsikos, D. and Cornell, C.A., Incremental dynamic analysis, *Earthquake Engineering and Structural Dynamics*, **31**, 491-514, 2002.